

# 1 Colored dissolved organic matter in shallow estuaries: relationships 2 between carbon sources and light attenuation

3 W. K. Oestreich<sup>1</sup>, N. K. Ganju<sup>2</sup>, J. W. Pohlman<sup>2</sup>, and S. E. Suttles<sup>2</sup>

4 <sup>1</sup>Department of Civil & Environmental Engineering, Northwestern University, Evanston, IL,  
5 USA

6 <sup>2</sup>U.S. Geological Survey Woods Hole Coastal and Marine Science Center, Woods Hole, MA,  
7 USA

8 Correspondence to: N. K. Ganju (nganju@usgs.gov)

9

## 10 Abstract

11 Light availability is of primary importance to the ecological function of shallow estuaries. For  
12 example, benthic primary production by submerged aquatic vegetation is contingent upon light  
13 penetration to the seabed. A major component that attenuates light in estuaries is colored  
14 dissolved organic matter (CDOM). CDOM is often measured via a proxy, fluorescing dissolved  
15 organic matter (fDOM), due to the ease of *in situ* fDOM sensor measurements. Fluorescence  
16 must be converted to CDOM absorbance for use in light attenuation calculations. However, this  
17 CDOM-fDOM relationship varies among and within estuaries. We quantified the variability in  
18 this relationship within three estuaries along the mid-Atlantic margin of the eastern United  
19 States: West Falmouth Harbor (MA), Barnegat Bay (NJ), and Chincoteague Bay (MD/VA).  
20 Land use surrounding these estuaries ranges from urban to developed, with varying sources of  
21 nutrients and organic matter. Measurements of fDOM (excitation and emission wavelengths of  
22 365nm ( $\pm 5$ nm) and 460nm ( $\pm 40$ nm), respectively) and CDOM absorbance were taken along a  
23 terrestrial-to-marine gradient in all three estuaries. The ratio of the absorption coefficient at  
24 340nm ( $m^{-1}$ ) to fDOM (QSU) was higher in West Falmouth Harbor (1.22) than in Barnegat Bay  
25 (0.22) and Chincoteague Bay (0.17). The CDOM:fDOM absorption ratio was variable between  
26 sites within West Falmouth Harbor and Barnegat Bay, but consistent between sites within  
27 Chincoteague Bay. Stable carbon isotope analysis for constraining the source of dissolved  
28 organic matter (DOM) in West Falmouth Harbor and Barnegat Bay yielded  $\delta^{13}C$  values ranging

1 from -19.7‰ to -26.1‰ and -20.8‰ to -26.7‰, respectively. Concentration and stable carbon  
2 isotope mixing models of DOC (dissolved organic carbon) indicate a contribution of  $^{13}\text{C}$ -  
3 enriched DOC in the estuaries. The most likely source of  $^{13}\text{C}$ -enriched DOC for the systems we  
4 investigated is *Spartina* cordgrass. Comparison of DOC source to CDOM-fDOM absorption  
5 ratios at each site demonstrates the relationship between source and optical properties. Samples  
6 with  $^{13}\text{C}$ -enriched carbon isotope values, indicating a greater contribution from marsh organic  
7 material, had higher CDOM-fDOM absorption ratios than samples with greater contribution  
8 from terrestrial organic material. Applying a uniform CDOM-fDOM absorption ratio and  
9 spectral slope within a given estuary yields errors in modeled light attenuation ranging from 11-  
10 33% depending on estuary. The application of a uniform absorption ratio across all estuaries  
11 doubles this error. This study demonstrates that light attenuation coefficients for CDOM based  
12 on continuous fDOM records are highly dependent on the source of DOM present in the estuary.  
13 Thus, light attenuation models for estuaries would be improved by quantification of CDOM  
14 absorption and DOM source identification.

15

## 16 **1 Introduction**

17 Benthic primary production in estuaries, including those along the Atlantic coast of the United  
18 States, is typically dominated by seagrass (Heck et al., 1995). Furthermore, seagrass acts as an  
19 ecosystem engineer in temperate coastal ecosystems via habitat provision and nutrient cycling  
20 (Ehlers et al. 2008). Recent anthropogenic nutrient loading to these ecosystems due to industrial  
21 and agricultural development has caused a loss of seagrass density. This occurs as eutrophication  
22 creates water column algal blooms and increases benthic algae populations (Burkholder et al.,  
23 2007; Hauxwell et al., 2003). These algal processes reduce penetration of the light necessary for  
24 survival of seagrasses. As anthropogenic impacts on coastal ecosystems compound with  
25 increasing urbanization of coastal zones (McGranahan et al., 2007), it is important to understand  
26 the factors controlling light attenuation in the estuarine water column.

27 Four main factors attenuate light in the water column: water itself, non-algal particulate material,  
28 phytoplankton, and colored dissolved organic matter (CDOM) (Kirk, 1994). Proxies are typically  
29 used to quantify these factors *in situ*: depth, turbidity, chlorophyll-a fluorescence, and  
30 fluorescing dissolved organic matter (fDOM), respectively (Ganju et al. 2014). The use of fDOM

1 as a proxy for the CDOM component is widespread due to the ease of measuring *in situ*  
2 fluorescence. However, variability in the CDOM-fDOM absorption ratios observed both between  
3 and within numerous aquatic systems (Clark et al., 2004; Del Castillo et al. 1999; Hoge et al.  
4 1993) confounds using fDOM alone to quantify absorbance. Quantifying and understanding what  
5 controls the relationship between fDOM and CDOM is required to accurately model light  
6 attenuation and seagrass viability in estuaries. CDOM also has great importance for its utility as  
7 a tracer (Stedmon et al., 2003; Del Castillo et al., 1999), its major role in photochemistry  
8 (Mopper et al., 2015), its effects on biological production (Coble, 2007), and remote sensing  
9 relevance (Nelson and Siegel, 2013).

10 Estuaries are transition zones between freshwater and marine systems where DOM from a  
11 variety of sources mixes (Raymond and Bauer, 2001). The major sources of DOM to estuaries  
12 are typically terrestrial DOM from riverine inputs, oceanic DOM from phytoplankton, and tidal  
13 marsh DOM from emergent and submergent marsh vegetation (Peterson et al., 1994). Both  
14 seagrass and macroalgae can also contribute DOM in these systems (Barron et al., 2014;  
15 Pregnall, 1983). Marine and terrestrial DOM exhibit different structural characteristics (Harvey  
16 et al., 1983) that are reflected in the optical properties of CDOM (Helms et al., 2008; De Souza  
17 Sierra et al., 1994). Additionally, photodegradation is a major sink for CDOM (Mopper et al.,  
18 2015; Kouassi and Zika, 1992), and must also be considered when discussing CDOM and light  
19 attenuation. Due to its role in attenuating light in the water column, measurement of CDOM and  
20 enhanced understanding of its source-dependent optical properties is important for modeling  
21 light availability in estuaries.

22 The goal of this study is to improve the understanding of light attenuation in the estuarine water  
23 column by characterizing the optical properties and sources of CDOM in three diverse estuaries  
24 located along the mid-Atlantic US margin: West Falmouth Harbor (MA), Barnegat Bay (NJ),  
25 and Chincoteague Bay (MD, VA). Our objectives are to quantify the CDOM-fDOM absorption  
26 ratio, establish absorption spectral slopes for use in light models (Gallegos et al., 2011),  
27 determine the sources of CDOM in these estuaries, and identify variation in the CDOM-fDOM  
28 absorption ratio as a function of source.

29

## 30 **2 Site Descriptions**

## 1   **2.1   West Falmouth Harbor**

2   West Falmouth Harbor is a small (0.7 km<sup>2</sup>), groundwater-fed estuary on the western shore of  
3   Cape Cod, Massachusetts (Fig. 1b). The harbor has a mean depth of approximately 1 m, and is  
4   connected to Buzzard's Bay by a 3-m deep, 150-m wide channel. Residence time in the harbor is  
5   approximately one day (Hayn et al., 2014). Tidal range is 1.9 m during spring tides and 0.7 m  
6   during neap tides, with tidal currents at the mouth approaching 0.5 m/s. The dominant source of  
7   freshwater and nutrients is groundwater. Land use surrounding the harbor is largely residential,  
8   with influence from a legacy wastewater plume within the aquifer (Ganju et al., 2012). Plant  
9   coverage in surrounding wetlands is variable, but *Spartina alterniflora* and *Spartina patens* tend  
10   to dominate, with some lesser coverage by *Juncus gerardi* and forbs such as *Salicornia* spp.,  
11   *Limonium carolinianum*, and *Solidago sempervirens* (Buchsbaum and Valiela, 1987). *Zostera*  
12   spp. eelgrass is also present in the harbor (Del Barrio et al., 2014).

## 13   **2.2   Barnegat Bay**

14   The Barnegat Bay-Little Egg Harbor estuary is a back-barrier system along the New Jersey  
15   Atlantic coast (Fig. 1c). The estuary is approximately 70 km long, 2-6 km wide, and 1.5 m deep.  
16   Bay and ocean water exchange occurs at three inlets: the Point Pleasant Canal at the northern  
17   limit, Barnegat Inlet in the middle of the barrier island, and Little Egg Inlet at the southern limit.  
18   Limited exchange through these inlets leads to a spatially variable residence time exceeding 30 d  
19   in some locations (Defne and Ganju, 2014). For the purpose of this study, sites north of Barnegat  
20   Inlet are referred to as "North Barnegat Bay," while sites parallel to and south of Barnegat Inlet  
21   are referred to as "South Barnegat Bay." Tides are semidiurnal and range from <0.1-1.5 m, and  
22   current velocities range from <0.5-1.5 m/s (Kennish et al., 2013; Ganju et al., 2014); there is also  
23   a pronounced south-to-north gradient in tidal range and flushing (Defne and Ganju, 2014). While  
24   the land surrounding the northern portion of the bay is developed with mixed urban-residential  
25   land use, the area south of Barnegat Inlet is less developed and retains much of the original  
26   marsh (Wieben and Baker, 2009). The salt marshes south of Barnegat Inlet are dominated by  
27   *Spartina alterniflora* (Olsen and Mahoney, 2001). Freshwater inputs are largest at the northern  
28   end of the bay due to the Toms River, Metedeconk River, and Cedar Creek (U.S. EPA, 2007).

## 29   **2.3   Chincoteague Bay**

1 Chincoteague Bay is along the Atlantic coast of the Delmarva Peninsula (Fig. 1d). This estuary  
2 has an area of 355 km<sup>2</sup> and an average depth of 2 m. The watershed surrounding Chincoteague  
3 Bay is 487 km<sup>2</sup>, and consists of 36% forest, 31% agricultural development, 25% wetlands, and  
4 8% urban development (Bricker et al., 1999). Vegetation in the wetland portion is dominated by  
5 *Spartina alterniflora*, much like South Barnegat Bay (Keefe and Boynton, 1973). Tide range  
6 averages 0.5 m, and residence time has been estimated at 8 days (Bricker et al., 1999). The Bay  
7 is connected to the ocean via two inlets: Ocean City Inlet in the north and Chincoteague Inlet in  
8 the south (Allen et al., 2007). Historically, Chincoteague Bay has been marked by extensive  
9 seagrass coverage and higher water quality, especially compared to other more developed and  
10 less well-flushed bays on the Atlantic coast (Wazniak et al., 2004).

### 11 **3 Methods**

#### 12 **3.1 Fluorescence measurements**

13 Sampling sites were approached by both land (WF01-WF13, BB01-BB07) and sea (BB08-BB16,  
14 CB01-CB10). Sampling occurred from June 25, 2014 to July 17, 2014 (Table 1). Either a bucket  
15 (sites approached on foot) or one-liter Nalgene sampling bottle (sites approached by boat) was  
16 rinsed with native water and then used to collect a surface water sample. A pre-calibrated YSI  
17 EXO 2 multisonde, measuring fDOM, temperature, salinity, pH, turbidity, chlorophyll-a  
18 fluorescence, blue-green algae fluorescence, and dissolved oxygen concentration was placed in  
19 each sample. Excitation and emission wavelengths for the fluorescing dissolved organic matter  
20 sensor were 365nm (±5nm) and 460nm (±40nm), respectively. Measurements of each parameter  
21 were collected at 1 s intervals for approximately 60 s and averaged. For sites approached on foot,  
22 the YSI EXO was deployed immediately; for sites approached by boat, the YSI EXO was  
23 deployed later on land (in concurrence with absorbance measurements, as described below).

24 Temperature, turbidity, and inner filter effects (IFE) have been shown to alter fluorescence  
25 measurements (Baker, 2005; Downing et al., 2012). For this reason, we corrected fluorescence  
26 measurements to account for temperature, turbidity, and IFE, according to Downing et al. (2012).

#### 27 **3.2 Absorbance measurements**

28 A 60-ml syringe was used to draw a water sample from these buckets for absorbance  
29 measurements. Fifteen ml of this sample was filtered through a 0.2-µm inorganic membrane

1 filter into a 5-cm path length cuvette. Absorbance measurements were recorded in 20-nm  
 2 increments over the range of 340-440 nm (West Falmouth Harbor) or 340-720 nm (Barnegat Bay  
 3 and Chincoteague Bay). Spectral slope was calculated over both the entire 340-720 nm range and  
 4 the 340-440 nm range for Barnegat Bay and Chincoteague Bay to allow for direct comparison to  
 5 West Falmouth Harbor and other studies (e.g., Huang and Chen, 2009; Del Castillo et al., 1999).  
 6 The estimated photometric accuracy of the spectrophotometer was 0.003 absorbance units.  
 7 Offsets from zero were determined for the WFH CDOM spectra by running a blank sample  
 8 (Milli-Q water) at 440nm (the high end of the recorded spectrum). For BB and CB, offsets from  
 9 zero were determined by running a blank sample before measurement at each wavelength (340-  
 10 720nm). Absorbance measurements were converted to Napierian absorption coefficients as  
 11 follows:

$$12 \quad a(\lambda) = 2.303A(\lambda)/l \quad (1)$$

13 where  $A(\lambda)$  is the absorbance at 340 nm,  $l$  is the cell length in meters (0.05 m for this study), and  
 14  $a(\lambda)$  is the absorption coefficient (Green and Blough, 1994). 340 nm had the highest absorbance  
 15 values across the range scanned and therefore was chosen as the absorbance wavelength for  
 16 calculating the absorbance coefficient. Spectral slopes were calculated by plotting the natural log  
 17 of absorption coefficient against wavelength. Due to use of the natural log, non-positive  
 18 absorption coefficients were discarded to calculate spectral slope, as described in Equation 2  
 19 (Bricaud et al., 1981):

$$20 \quad S = \ln(a(\lambda)/a(r))(r - \lambda) \quad (2)$$

21 where  $\lambda$  is wavelength,  $r$  is a reference wavelength,  $a(\lambda)$  is absorption coefficient at a given  
 22 wavelength,  $a(r)$  is absorption coefficient at the reference wavelength, and  $S$  is the spectral slope.  
 23 The value of  $S$  shows the rate at which absorption decreases with increasing wavelength (Green  
 24 and Blough, 1994). This parameter can be used to predict absorption coefficients across the  
 25 spectrum based on absorption at one reference wavelength (Bricaud et al., 1981).

### 26 **3.3 Isotope Analysis**

27 At each site in West Falmouth Harbor and Barnegat Bay, water samples were collected for stable  
 28 carbon isotope analysis of DOC (dissolved organic carbon). Chincoteague Bay was excluded  
 29 due to logistical limitations. 30 ml of the collected sample was filtered through a 0.2- $\mu$ m

1 inorganic membrane filter, collected in a 40-ml glass autosampler vial that had been baked at 450  
2 °C for 4 hours and sealed with caps and Teflon-faced silicon septa that had been soaked and  
3 rinsed with 10% (by volume) HCl. Additionally, trace metal grade 12N HCl (Sigma Aldrich)  
4 was added to each isotope water sample to achieve pH<2. The vials were then stored at 4 °C.  
5 Samples were analyzed by High Temperature Combustion - Isotope Ratio Mass Spectrometry  
6 (HTC-IRMS) at the USGS-WHOI Dissolved Carbon Isotope Lab (DCIL), as described by  
7 Lalonde et al. (2014). The DCIL HTC-IRMS system consists of an OI 1030C Total Carbon  
8 Analyzer and a Graden molecular sieve trap interfaced to a Thermo-Finnigan DeltaPlusXP IRMS  
9 via a modified Conflo IV. The stable carbon isotope ratios are reported in the standard  $\delta$ -  
10 notation relative to Vienna Pee Dee Belemnite (VPDB) and are corrected by mass balance to  
11 account for the analytical blank, which was less than the equivalent of 15  $\mu$ M DOC in the  
12 sample. By comparison, the sample DOC concentrations ranged from 60.7 to 581  $\mu$ M. Thus the  
13 blank correction was always less than 25% of the sample concentration. The analytical precision  
14 of the  $\delta^{13}\text{C}$  analysis was less than 0.3‰. DOC concentration was calculated using a standard  
15 curve consisting of four potassium hydrogen phthalate (KHP) calibration standards quantified as  
16 the integrated volt-seconds (Vs) of the mass-44 peak on the IRMS (Lalonde et al., 2014). Peak  
17 areas were corrected for analytical blanks determined from ultrapure lab water injections.

18 Salinity and  $\delta^{13}\text{C}$  values for freshwater and marine end-members from West Falmouth Harbor  
19 and Barnegat Bay were used to construct isotope mixing models for the estuaries (Kaldy et al.,  
20 2005). Marine and freshwater end-members are defined as the most and least saline samples  
21 collected at each estuary. Because of the number of samples clustered near the highest salinity  
22 for each estuary, marine end-members were checked with geographic location. For West  
23 Falmouth Harbor, the site chosen as marine end-member (WF01) was taken from the mouth of  
24 the harbor where the estuary connects to Buzzard's Bay. For Barnegat Bay, the site of highest  
25 salinity (BB13) was taken from the middle of Little Egg Harbor in South Barnegat Bay.

26 However, a more geographically intuitive marine end-member would be site BB16, near Little  
27 Egg Inlet. The only slightly lower salinity at this site (29.69 psu) as compared to BB13 (30.08  
28 psu), along with the geographic location of BB16 at an oceanic inlet, makes BB16 a more  
29 appropriate marine end-member. Therefore, end-members used in the conservative mixing  
30 models were as follows: WF06 (freshwater), WF01 (marine), BB01 (freshwater), and BB16  
31 (marine). The conservative mixing models (Kaldy et al., 2005) were constructed as:

$$1 \quad C_{mix} = fC_R + (1 - f)C_O \quad (3)$$

2 where  $C_{mix}$  is the calculated concentration for use in the mixing model,  $C_R$  and  $C_O$  are freshwater  
3 and marine end-member DOC concentrations, respectively, and  $f$  is the fraction of freshwater  
4 calculated from salinity:

$$5 \quad f = (S_O - S_M)/(S_O - S_R) \quad (4)$$

6 where  $S_M$  is measured salinity at a specific site, and  $S_R$  and  $S_O$  are freshwater and marine end-  
7 member salinities, respectively. These calculations lead to the modeled isotope ratio of each  
8 sample as:

$$9 \quad \delta_{mix} = [fC_R \delta_R + (1 - f)C_O \delta_O]/C_{mix} \quad (5)$$

10 where all subscripts and variables are the same as described for Eq. 3 and 4.

### 11 **3.4 Carbon-normalized CDOM**

12 In addition to the stable carbon isotope analysis, a “carbon-normalized CDOM” (C-normalized  
13 CDOM<sub>340</sub>) was calculated for each sample as:

$$14 \quad C\text{-normalized } CDOM_{340} = A(\lambda)/DOC \quad (6)$$

15 where  $DOC$  is dissolved organic carbon concentration (mg/L) and  $A(\lambda)$  is Decadic light  
16 absorbance at 340 nm ( $m^{-1}$ ). This C-normalized CDOM<sub>340</sub> is comparable to Specific Ultraviolet  
17 Absorbance (SUVA), a measure proven to correlate strongly with DOC aromaticity (Weishaar et  
18 al., 2003). While SUVA is typically calculated at 254 nm, the C-normalized CDOM<sub>340</sub> calculated  
19 here provides a similar measure while accommodating this study’s minimum absorbance  
20 measurement wavelength of 340 nm.

## 21 **4 Results**

### 22 **4.1 Spectral slopes**

23 The estuary-wide average spectral slope (over the range 340-440 nm) for West Falmouth was  
24 steeper than for Barnegat and Chincoteague, with  $S_{avg}$  equal to 0.021, 0.016, and 0.018,  
25 respectively (Table S1). At West Falmouth Harbor, spectral slope ranged from 0.013 – 0.044,  
26 with a standard deviation of 0.010. At Barnegat Bay,  $S$  ranged from 0.011 – 0.019, with a  
27 standard deviation of 0.002. At Chincoteague Bay,  $S$  ranged from 0.014 – 0.023, with a standard



1 deviation of 0.003. Spectral slope values for Barnegat and Chincoteague were slightly steeper  
2 over the range 340-440 nm as compared to  $S$  calculated over the range 340-720 nm (Table S1).

### 3 **4.2 Fluorescence measurements (fDOM)**

4 At West Falmouth, fDOM ranged from 0.63 – 10.21 QSU, with a standard deviation of 2.57  
5 QSU. At Barnegat Bay, fDOM ranged from 12.06 – 84.40 QSU, with a standard deviation of  
6 20.82 QSU. At Chincoteague Bay, fDOM ranged from 11.15 – 49.49 QSU, with a standard  
7 deviation of 10.95 QSU. Values observed for fDOM were within ranges reported for similar  
8 estuaries and coastal waters (Callahan et al., 2004; Clark et al., 2002; Green and Blough, 1994).  
9 Sites at West Falmouth and Barnegat Bay represented a freshwater to seawater gradient, with  
10 salinity ranging from 0.13 – 31.28 psu at West Falmouth and 3.41 – 30.08 psu at Barnegat. At  
11 Chincoteague Bay, salinity ranged from 25.88 – 31.85 psu. A complete salinity gradient was not  
12 sampled at Chincoteague due to the relatively high salinity found throughout the main basin of  
13 the bay, and low freshwater input. fDOM correlated inversely with salinity (Fig. 2), as expected  
14 because riverine input is typically the main external source of DOM. However, the slope and  
15 strength of the fDOM-salinity relationship differed both between and within estuaries. The  
16 steepest relationship (most rapidly decreasing fDOM signal with increasing salinity) was  
17 observed at Chincoteague Bay and in South Barnegat Bay. These two areas displayed a similar  
18 fDOM-salinity relationship, fDOM and salinity showed a slightly less negative relationship at  
19 South Barnegat Bay, and even less negative at West Falmouth Harbor.

### 20 **4.3 CDOM absorption and CDOM-fDOM ratios**

21 At West Falmouth,  $a(340)$  ranged from 0.92 – 5.07  $\text{m}^{-1}$ , with a standard deviation of 1.02  $\text{m}^{-1}$ . At  
22 Barnegat Bay,  $a(340)$  ranged from 0.97 – 14.97  $\text{m}^{-1}$ , with a standard deviation of 3.99  $\text{m}^{-1}$ . At  
23 Chincoteague Bay,  $a(340)$  ranged from 1.84 – 8.38  $\text{m}^{-1}$ , with a standard deviation of 1.86  $\text{m}^{-1}$   
24 (Table 2). The ratio between  $a(340)$  and fDOM differed both between and within estuaries, as  
25 expected (Table S1; Fig. 3). The mean ratio of  $a(340)$  to fDOM was relatively higher in West  
26 Falmouth Harbor (1.22) than in Barnegat Bay (0.22) and Chincoteague Bay (0.17). There were  
27 two significant outliers at Barnegat Bay: BB01, which had a lower absorption coefficient (0.97  
28  $\text{m}^{-1}$ ) than expected based on its higher fDOM value (69.92 QSU); and BB15, which showed a  
29 much higher absorption coefficient (14.97  $\text{m}^{-1}$ ) than expected based on its lower fDOM value

1 (16.50 QSU). West Falmouth also demonstrated substantial variability in  $a(340)/fDOM$  ratio  
2 between sites. Chincoteague Bay however, showed a highly consistent ratio.

### 3 **4.4 Stable carbon isotope analysis**

4 The observed isotope-salinity relationship at West Falmouth Harbor and Barnegat Bay had  
5 numerous  $\delta^{13}C$  values well outside the range predicted by concentration and isotopic  
6 conservative mixing models (Table S2; Figs. 4a and 5a), which suggests an additional DOM  
7 source from within the estuaries (discussed further in Section 5.3). For West Falmouth Harbor,  
8 end-members of the conservative mixing model had  $\delta^{13}C$  values of -23.0‰ and -26.1‰. The  
9 observed  $\delta^{13}C$  data however, ranged from -19.7‰ to -26.1‰, six of which were more  $^{13}C$ -  
10 enriched samples than the modeled range. For Barnegat Bay, end-members of the conservative  
11 mixing model had  $\delta^{13}C$  values of -22.1‰ and -26.7‰. The observed  $\delta^{13}C$  data ranged from -  
12 20.8‰ to -26.7‰, four of which were more  $^{13}C$ -enriched than the modeled range. The two  
13 points from North Barnegat Bay falling well above the model (Fig. 5a) correspond to sites BB04  
14 and BB09. The two points from South Barnegat Bay falling well above the model correspond to  
15 sites BB12 and BB14. These  $^{13}C$ -enriched samples from Barnegat were all taken from areas near  
16 significant stretches of marsh along the western edge of Barnegat Bay. Furthermore, these  
17 samples all fall above the concentration-based mixing model for Barnegat Bay (Fig. 5b). Spatial  
18 representation of  $\delta^{13}C$  values at Barnegat Bay (Fig. 5c) shows significantly less negative  $\delta^{13}C$   
19 values in South Barnegat Bay compared to North Barnegat Bay.

### 20 **4.5 Comparison of isotopic signature and fDOM-CDOM absorption ratio**

21 Comparison of the isotopic and optical analyses suggests a correlation between  $\delta^{13}C$  signature  
22 and fDOM-CDOM absorption ratio (Fig. 6). For both West Falmouth Harbor and Barnegat Bay,  
23 the more  $^{13}C$ -enriched samples also had a higher absorption coefficient per unit fluorescence.  
24 This trend is highlighted by the extremes of the dataset, with the most  $^{13}C$ -enriched sample  
25 (WF02) displaying the highest CDOM-fDOM absorption ratio, and the least  $^{13}C$ -enriched sample  
26 (BB01) displaying the lowest CDOM-fDOM absorption ratio. Furthermore, West Falmouth  
27 Harbor samples had both higher CDOM-fDOM absorption ratios (-0.032, natural log scale,  
28 average) and  $^{13}C$  enrichment ( $\delta^{13}C$  average of -22.4‰) as compared to Barnegat Bay (-1.75 and -  
29 23.4‰, respectively).

1

## 2 **5 Discussion**

### 3 **5.1 Absorption coefficient and spectral slope ranges**

4 Absorption coefficients for West Falmouth and Chincoteague were comparable to those reported  
5 for other estuaries and coastal waters (Chen et al., 2003; Green and Blough, 1994). Absorption  
6 coefficients for Barnegat Bay were somewhat higher, but within the range reported by Green and  
7 Blough (1994). Likewise, all values observed for spectral slope were within ranges reported for  
8 similar estuaries and coastal waters (Keith et al., 2002; Green and Blough, 1994), despite  
9 differences in the range over which spectral slope was calculated (400–550 nm for Keith et al.,  
10 2002; 290nm to wavelength of absorption detection limit for Green and Blough, 1994). At  
11 Barnegat Bay and Chincoteague Bay, the range of calculated spectral slopes was quite small  
12 (Table S1). At West Falmouth Harbor, however, there was significantly more variability in  
13 spectral slope. West Falmouth Harbor is a relatively dynamic system with multiple freshwater  
14 point sources and unique mixing characteristics (Ganju et al., 2012). Considering the dramatic  
15 influence that variable sources (aquatic vs. terrestrial) and alterations (e.g. microbial and  
16 photodegradation) have on the optical properties of DOM (Spencer et al., 2009; Helms et al.,  
17 2008; De Souza Sierra et al., 1994) the variability in spectral slopes observed at West Falmouth  
18 Harbor may be attributable to the physical complexity and short residence time of this estuary.  
19 More specifically with respect to source, previous studies have shown that DOM comprised of  
20 primarily fulvic acids has steeper spectral slopes than DOM comprised of primarily humic acids  
21 (Carder et al., 1989). Considering the physical complexity and variety of point sources at West  
22 Falmouth Harbor, variable organic matter composition and spectral slope is not surprising.

### 23 **5.2 Variability in fDOM-salinity relationship**

24 The inverse relationship between fDOM and salinity observed for these three estuaries is  
25 consistent with other estuarine studies (Clark et al., 2002; Green and Blough, 1994). Differing  
26 slopes of the inverse relationships suggests the freshwater DOM sources vary between and  
27 within estuaries. This is due to differences in organic matter composition and fluorescence  
28 between the freshwater sources (Stedmon et al., 2003; Parlanti et al., 2000). South Barnegat Bay  
29 and Chincoteague Bay display a similar fDOM-salinity relationship, while South Barnegat Bay

1 and North Barnegat Bay show a divergent relationship. South Barnegat Bay and Chincoteague  
2 Bay also have geographic and land use similarities with less development and extensive *Spartina*  
3 *alterniflora*-dominated marshes (Wieben and Baker, 2009; Olsen and Mahoney, 2001; Keefe and  
4 Boynton, 1973), whereas North Barnegat Bay is much more developed (Wieben and Baker,  
5 2009). Furthermore, North and South Barnegat Bay appear to have different organic matter  
6 sources (determined via isotope analysis; see Section 5.3). This information considered together  
7 supports the idea of differing organic matter sources due to various inputs affecting fluorescence  
8 properties. As for the variability seen within West Falmouth Harbor, this is again likely  
9 attributable to the relatively low fluorescence signals observed throughout the estuary, along  
10 with the variety of freshwater inputs to this complex system.

### 11 **5.3 Evidence for internal DOM sources**

12 The disparity between observed  $\delta^{13}\text{C}$  values and those predicted by conservative mixing models  
13 (Figs. 4a and 5a) suggest an additional DOM source within the estuaries. Previous studies of  
14 DOC in eastern US estuaries have suggested a marine end-member  $\delta^{13}\text{C}$  value of -24‰ to -22‰,  
15 and a freshwater end-member  $\delta^{13}\text{C}$  of -28‰ to -26‰ (Peterson et al., 1994). Observed values  
16 falling above the mixing model and approaching much more  $^{13}\text{C}$ -enriched values than the  
17 defined marine end-member is likely due to the influence of DOC from *Spartina* spp. cordgrass  
18 in nearby salt marshes. Analysis of DOC *Spartina* spp. by past studies has indicated a  $\delta^{13}\text{C}$   
19 signature of about -16.4‰ to -11.7‰ (Komada et al., 2012; Chmura and Aharon, 1995). The  
20 tendency of values from this study towards this  $^{13}\text{C}$ -enriched signature, in combination with  
21 knowledge of *Spartina* coverage around the sites differing from conservative mixing models,  
22 suggests a DOM source derived from *Spartina* cordgrass. The influence of this end-member is  
23 particularly notable in South Barnegat Bay (specifically sites BB12 and BB14), where *Spartina*  
24 coverage is extensive (Olsen and Mahoney 2001), and the  $\delta^{13}\text{C}$  of the DOC is -21.6‰ and -  
25 20.9‰ for BB12 and BB14, respectively. Although *Spartina* coverage in North Barnegat Bay is  
26 not as extensive as in South Barnegat Bay, the sites with DOC  $\delta^{13}\text{C}$  values that are more  
27 enriched than the conservative mixing model for North Barnegat Bay (BB04 and BB09) were  
28 taken from inland sampling locations, specifically the north bank of the lower Toms River and  
29 Reedy Creek, where stands of *Spartina* are present.

1 However, the observed  $^{13}\text{C}$ -enrichment could also be attributed to *Zostera* eelgrass, which has  
2 been shown to exhibit a  $^{13}\text{C}$ -enriched signature (Hemminga and Mateo, 1996). For this reason,  
3 the aforementioned samples falling well above the conservative mixing models cannot  
4 necessarily be considered a result of *Spartina* influence. However, a comparison of site locations  
5 to known seagrass and *Spartina* wetland coverage can yield some indication of the most likely  
6 source of  $^{13}\text{C}$ -enriched DOC. Seagrass coverage maps (Lathrop and Haag, 2011) and maps of  
7 estuarine intertidal wetland coverage (U.S. Fish & Wildlife Service, 2015) for Barnegat Bay  
8 show intertidal wetland coverage and no seagrass coverage for sites BB09, BB12, and BB14.  
9 Site BB04 is characterized by neither coverage, but its inland location places it much closer to  
10 known intertidal wetland coverage (U.S. Fish & Wildlife Service, 2015). This geographic  
11 comparison indicates *Spartina* as the more likely additional end-member at Barnegat Bay,  
12 though *Zostera* influence is still possible. Considering the movement of water and potential for  
13 mixing during residence in the estuary, this geographic analysis is by no means definitive, but  
14 does provide some insights.

15 For West Falmouth Harbor, sites falling well above the conservative mixing model (WF02,  
16 WF03, WF04, WF05, WF07, WF11) were compared to known seagrass (Del Barrio et al., 2014)  
17 and intertidal wetland (U.S. Fish & Wildlife Service, 2015) coverage for West Falmouth Harbor.  
18 For sites WF03, WF05, WF07, and WF11, there is known intertidal wetland coverage and no  
19 known *Zostera* coverage. For site WF02, there is both intertidal wetland coverage and *Zostera*  
20 coverage, whereas WF04 corresponds to neither *Spartina* nor *Zostera*. This comparison yields a  
21 less clear picture of DOC sources, but this is to be expected considering the aforementioned  
22 complexity of surrounding land uses, potential DOC inputs, and limited mixing at West  
23 Falmouth Harbor. Furthermore, spatial representation of  $\delta^{13}\text{C}$  values at West Falmouth Harbor  
24 (Fig. 4c) show  $^{13}\text{C}$ -depleted samples in the northeastern corner of the harbor, the location of a  
25 freshwater culvert discharging groundwater (Ganju, 2011). On the whole, the conservative  
26 mixing models used in this study may not be appropriate for a system as complex as West  
27 Falmouth Harbor. Unlike the clear indication of a third end-member from the mixing model for  
28 Barnegat Bay, one could envision a more complex system with multiple additional end-members  
29 for West Falmouth Harbor (Fig. 4a and 4b).

30

## 1 **5.4 Potential influence of photodegradation**

2 We also considered the potential influence of photodegradation on the samples with DOC that  
3 was  $^{13}\text{C}$ -enriched in comparison to the conservative mixing model. Irradiation experiments have  
4 shown that riverine DOC becomes  $^{13}\text{C}$ -enriched by  $\sim 3.5\%$  and concentrations decrease by as  
5 much as 45% over 57 days as a result of photodegradation (Spencer et al., 2009), suggesting the  
6 possibility that the aforementioned  $^{13}\text{C}$ -enriched samples are photodegraded terrestrial DOM.  
7 This is unlikely for samples from West Falmouth Harbor, given the very short residence time of  
8 this estuary ( $\sim 1$  day; Hayn et al., 2014). For Barnegat Bay however, the influence of  
9 photodegradation is possible. Sites BB12 and BB14 are in areas with residence time of  $\sim 10$  days,  
10 while sites BB04 and BB09 are in areas with residence time of  $\sim 15$ -20 days (Defne and Ganju,  
11 2014). These residence times are within the timeframe over which photodegradation effects on  
12  $\delta^{13}\text{C}$  have previously been observed (Spencer et al., 2009), which could also influence the  $^{13}\text{C}$ -  
13 enriched signatures observed for these samples. However, the relative lack of  $^{13}\text{C}$ -enrichment  
14 observed at other Barnegat Bay sites with even longer residence times (e.g. BB03 and BB07;  
15 Defne and Ganju, 2014) implies that photodegradation alone likely does not explain the  $^{13}\text{C}$ -  
16 enriched signatures found for certain Barnegat Bay samples. Furthermore, and most convincing,  
17 the concentration-based mixing model for Barnegat Bay (Fig. 5b) demonstrates a net input of  
18 DOC into the estuary. DOC concentrations that exceed the conservative concentration-based  
19 mixing model indicate a source of DOC within the estuary. If the samples were affected by  
20 photodegradation, one would expect a net loss of measured DOC within the estuary (e.g.,  
21 Spencer et al., 2009).

22 Further insight on the possibility of photodegradation can be derived from the C-normalized  
23  $\text{CDOM}_{340}$  (Table S2). Carbon-normalized CDOM correlates strongly with sample aromaticity  
24 (Weishaar et al., 2003), which one would expect to decrease as a result of photodegradation  
25 (Hood et al., 2005). However, C-normalized  $\text{CDOM}_{340}$  (and thus aromaticity) is not significantly  
26 lower for the potentially photodegraded terrestrial DOM samples as compared to other terrestrial  
27 DOM samples such as BB01 and BB03 (Table S2). This lack of a drop in aromaticity does not  
28 support the possibility that the  $^{13}\text{C}$ -enriched samples from Barnegat Bay are photodegraded  
29 terrestrial DOM.

## 30 **5.5 Variability in fDOM-CDOM absorption relationship**

1 The variability between fDOM and CDOM absorption in these estuaries was expected based on  
2 the results of previous studies (Clark et al., 2004; Del Castillo et al., 1999; Hoge et al., 1993).  
3 West Falmouth Harbor in particular showed a different absorption coefficient to fDOM ratio as  
4 compared to the general trend for Barnegat and Chincoteague Bays (Fig. 3). We ascribe this  
5 difference to groundwater inputs, which have been shown to have lower CDOM (Shen et al.,  
6 2015; Chen et al., 2010; Huang and Chen, 2009) and are substantial in WFH (Ganju, 2011).  
7 Additionally, the extremes of CDOM variability in this study can be explained by differing DOC  
8 sources within the estuaries. While the relatively uniform CDOM-fDOM relationship for  
9 Barnegat Bay results in clustering of Barnegat Bay samples (Fig. 6), this relationship is  
10 highlighted by both the Barnegat Bay outliers and the higher CDOMabs/fDOM observed for the  
11 more <sup>13</sup>C-enriched samples at West Falmouth Harbor. Points such as the outliers at Barnegat Bay  
12 are indicative of how the CDOM-fDOM relationship can be altered in an estuary with such  
13 diverse sources and transport mechanisms. This assertion of variable CDOM-fDOM relationship  
14 depending on source is supported by the findings of Tzortziou et al., 2008, which suggested that  
15 marsh-exported DOC has a lower fluorescence per unit absorbance as compared to humic DOC  
16 originating from a freshwater source. For the two extreme outliers, <sup>13</sup>C-enriched DOC (likely  
17 *Spartina* source) was associated with a lower fluorescence per unit absorbance. <sup>13</sup>C-depleted  
18 DOC (terrestrial source) was associated with a higher fluorescence per unit absorbance. While  
19 other studies have focused on differences in the fluorescence-absorbance relationship as a  
20 function of molecular weight (Belzile and Guo, 2006; Stewart and Wetzel, 1980), the  
21 combination of CDOM optical and isotopic analyses presented here provide a connection  
22 between CDOM source and optical characteristics, as suggested by Tzortziou et al., 2008.

23 The effects of *in situ* processing on absorption properties of DOM must also be considered here.  
24 In particular, photodegradation is known to reduce the absorbance of light by DOM (Spencer et  
25 al., 2009; Kouassi and Zika, 1992). Therefore, observations of higher fluorescence per unit  
26 absorbance could be a result of photochemical effects. However, the <sup>13</sup>C-enriched DOC samples  
27 discussed here exhibit lower fluorescence per unit absorbance than expected. This trend provides  
28 additional evidence refuting the aforementioned possibility that the <sup>13</sup>C-enriched samples from  
29 Barnegat Bay are photodegraded terrestrial DOM (Section 5.4).

## 30 **5.6 Ramifications for light attenuation modeling**

1 The variability of fDOM optical properties between and within estuaries has important  
2 consequences for light attenuation models. Continuous estimates of light attenuation are possible  
3 with continuous proxy measurements of turbidity (for sediment), chlorophyll-a fluorescence, and  
4 fDOM (Gallegos et al., 2011), but Ganju et al. (2014) found that light models can be highly  
5 sensitive to the CDOM-fDOM relationship, specifically in Barnegat Bay. We applied the light  
6 model of Gallegos et al. (2011) to the individual measurements of turbidity, chlorophyll-a  
7 fluorescence, and fDOM collected in this study. We explored two cases to calculate light  
8 attenuation: 1) use of the individual point CDOM-fDOM ratio and spectral slope from  
9 measurements; and 2) use of an estuary-wide average CDOM-fDOM ratio and spectral slope  
10 (model parameters related to sediment particles and chlorophyll were held constant to values  
11 reported in Ganju et al., 2014). Variation in the DOM properties led to average light attenuation  
12 errors ranging from 11 to 33% (Table 2), with individual site errors over 200% at sites with the  
13 highest deviation from the estuary mean (site BB01, at the landward end of Barnegat Bay). This  
14 suggests that constraining optical properties of the DOM pool is critical for light modeling, and  
15 that high variability within an estuary may confound use of spatially constant parameters.

16

## 17 **6 Conclusions**

18 This study shows that the CDOM absorption-fDOM relationship is variable both between and  
19 within West Falmouth Harbor, Barnegat Bay, and Chincoteague Bay, and depends upon DOM  
20 source. DOM that was  $^{13}\text{C}$ -enriched (higher  $\delta^{13}\text{C}$  values) also had a higher absorption coefficient  
21 per unit fluorescence. Additionally, fDOM-salinity relationship was variable between and within  
22 these estuaries. The exception here was the lack of variability in these relationships within  
23 Chincoteague Bay. Future work in relation to this study might involve a stable carbon isotope  
24 analysis at Chincoteague Bay similar to the analysis carried out here for West Falmouth Harbor  
25 and Barnegat Bay. Results of such an analysis could further elucidate the effects of DOM source  
26 on the CDOM-fDOM ratio. Finally, spectral slopes for use in light models were consistent  
27 between and within Barnegat and Chincoteague Bays, with more variability observed at West  
28 Falmouth Harbor.

29



## 1 **Acknowledgements**

2 Funding was provided by the Woods Hole Oceanographic Institution Summer Student  
3 Fellowship Program and the USGS Coastal and Marine Geology Program. Thanks to Dr. Brian  
4 Bergamaschi of the U.S. Geological Survey California Water Science Center for input on fDOM  
5 corrections. Thanks to the Rutgers University Marine Field Station, in particular Tom Malatesta  
6 and Roland Hagan, for field support at Barnegat Bay. Thanks also to Dr. Nicholas Nidzieko of  
7 the University of Maryland Horn Point Laboratory for field support at Chincoteague Bay. Patrick  
8 Dickhudt and Wally Brooks provided assistance with instrument preparation and running of  
9 stable carbon isotope analysis samples, respectively. Any use of trade, firm, or product names is  
10 for descriptive purposes only and does not imply endorsement by the U.S. Government.

## 11 **Author Contributions**

12 W.K.O. executed the sampling strategy and analyzed data. N.K.G. and J.W.P. designed the  
13 experiment and assisted in data interpretation. S.E.S. assisted in designing and executing the  
14 sampling strategy. All authors contributed to the drafting of the manuscript.

## 15 **References**

- 16 Allen, T. R., Tolvanen, H. T., Oertel, G. F., and McLeod, G. M.: Spatial characterization of  
17 environmental gradients in a coastal lagoon, Chincoteague Bay, *Estuaries and Coasts*, 30, 959-  
18 977, 2007.
- 19 Baker, A.: Thermal fluorescence quenching properties of dissolved organic matter, *Water Res*,  
20 39, 4405-4412, 2005.
- 21 Barron, C., Apostolaki, E. T., and Duarte, C. M.: Dissolved organic carbon fluxes by seagrass  
22 meadows and macroalgal beds, *Front Mar Sci*, 1, doi: 10.3389/fmars.2014.00042, 2014.
- 23 Belzile, C., and Guo, L.: Optical properties of low molecular weight and colloidal organic  
24 matter: Application of the ultrafiltration permeation model to DOM absorption and fluorescence,  
25 *Mar Chem*, 98, 183-196, 2006.
- 26 Bricaud, A., Morel, A., and Prieur, L.: Absorption by dissolved organic matter of the sea (yellow  
27 substance) in the UV and visible domains, *Limnol Oceanogr*, 26, 43-53, 1981.

- 1 Bricker, S. B., Clement, C. G., Pirhalla, D. E., Orlando, S. P., and Farrow, D. R. G.: National  
2 Estuarine Eutrophication Assessment: Effects of Nutrient Enrichment in the Nation's Esuaries,  
3 NOAA, National Ocean Service, Special Projects Office and the National Centers for Coastal  
4 Ocean Science. Silver Spring, MD: 71 pp., 1999.
- 5 Buchsbaum, R., and Valiela, I.: Variability in the chemistry of estuarine plants and its effect on  
6 feeding by Canada geese. *Oecologia*, 73, 146-153, 1987.
- 7 Burkholder, J. M., Tomasko, D. A., and Touchette, B. W.: Seagrasses and eutrophication, *J Exp*  
8 *Mar Biol Ecol*, 350, 46-72, 2007.
- 9 Callahan, J., Dai, M., Chen, R. F., Li, X., Lu, Z., and Huang, W.: Distribution of dissolved  
10 organic matter in the Pearl River Estuary, China, *Mar Chem*, 89, 211-224, 2004.
- 11 Chen, C., Shi, P., Yin, K., Pan, Z., Zhan, H., and Hu, Z.: Absorption coefficient of yellow  
12 substance in the Pearl River estuary, *Proc. SPIE 4892, P Soc Photo-Opt Ins*, 215, 2003.
- 13 Chen, M., Price, R. M., Yamashita, Y., and Jaffe, R.: Comparative study of dissolved organic  
14 matter from groundwater and surface water in the Florida coastal Everglades using multi-  
15 dimensional spectrofluorometry combined with multivariate statistics, *Applied Geochemistry*,  
16 25, 872-880, 2010.
- 17 Chmura, G. L., and Aharon, P.: Stable carbon isotope signatures of sedimentary carbon in coastal  
18 wetlands as indicators of salinity regime, *J Coast Res*, 11, 124-135, 1995.
- 19 Clark, C. D., Jimenez-Morais, J., Jones II, G., Zanardi-Lombardo, E., Moore, C. A., and Zika, R.  
20 G.: A time-resolved fluorescence study of dissolved organic matter in a riverine to marine  
21 transition zone, *Mar Chem*, 78, 121-135, 2002.
- 22 Clark, C. D., Hiscock, W. T., Millero, F. J., Hitchcock, G., Brand, L., Miller, W. L., Ziolkowski,  
23 L., Chen, R. F., and Zika, R. G.: CDOM distribution and CO<sub>2</sub> production on the Southwest  
24 Florida Shelf, *Mar Chem*, 89, 145-167, 2004.
- 25 Coble, P. G.: Marine optical biogeochemistry: the chemistry of ocean color, *Chem Rev*, 107 (2),  
26 pp 402-418, 2007.

- 1 Defne, Z., and Ganju, N. K.: Quantifying the residence time and flushing characteristics of a  
2 shallow, back-barrier estuary: application of hydrodynamic and particle tracking models,  
3 *Estuaries and Coasts*, 1-16, doi: 10.1007/s12237-014-9885-3, 2014.
- 4 De Souza Sierra, M. M., Donard, O. F. X., Lamotte, M., Belin, C., and Ewald, M.: Fluorescence  
5 spectroscopy of coastal and marine waters, *Mar Chem*, 47, 127-144, 1994.
- 6 Del Barrio, P., Ganju, N. K., Aretxabaleta, A. L., Hayn, M., Garcia, A., and Howarth, R. W.:  
7 Modeling future scenarios of light attenuation and potential seagrass success in a eutrophic  
8 estuary, *Estuar Coast Shelf S*, 149, 13-23, 2014.
- 9 Del Castillo, C. E., Coble, P. G., Morell, J. M., Lopez, J. M., and Corredor, J. E.: Analysis of  
10 optical properties of the Orinoco River plume by absorption and fluorescence spectroscopy, *Mar*  
11 *Chem*, 66, 35-51, 1999.
- 12 Downing, B. D., Pellerin, B. A., Bergamaschi, B. A., Saraceno, J. F., and Kraus, T. E. C.: Seeing  
13 the light: The effects of particles, dissolved materials, and temperature on in situ measurements  
14 of DOM fluorescence in rivers and streams, *Limnol Oceanogr-Meth*, 10, 767-775, 2012.
- 15 Ehlers, A., Worm, B., and Reusch, T. B. H.: Importance of genetic diversity in eelgrass *Zostera*  
16 *marina* for its resilience to global warming, *Mar Ecol-Prog Ser*, 355, 1-7, 2008.
- 17 Gallegos, C. L., Werdell, P. J., and McClain, C. R.: Long-term changes in light scattering in  
18 Chesapeake Bay inferred from Secchi depth, light attenuation, and remote sensing  
19 measurements, *J Geophys Res*, 116, C00H08, DOI 10.1029/2011JC007160, 2011.
- 20 Ganju, N. K.: A novel approach for direct estimation of fresh groundwater discharge to an  
21 estuary, *Geophys Res Lett*, 38 (11), 2011.
- 22 Ganju, N. K., Hayn, M., Chen, S. N., Howarth, R. W., Dickhudt, P. J., Aretxabaleta, A. L., and  
23 Marino, R.: Tidal and groundwater fluxes to a shallow, microtidal estuary: Constraining inputs  
24 through field observations and hydrodynamic modeling, *Estuaries and Coasts*, 35, DOI  
25 10.1007/s12237-012-9515-x, 2012.
- 26 Ganju, N. K., Miselis, J. L., and Aretxabaleta, A. L.: Physical and biogeochemical controls on  
27 light attenuation in a eutrophic, back-barrier estuary, *Biogeosciences*, 11, 7193-7205,  
28 doi:10.5194/bg-11-7193-2014, 2014.

- 1 Green, S.A., and Blough, N. V.: Optical absorption and fluorescence properties of chromophoric  
2 dissolved organic matter in natural waters, *Limnol Oceanogr*, 39, 1903-1916, 1994.
- 3 Hauxwell, J., Cebrián, J., Valiela, I.: Eelgrass *Zostera marina* loss in temperate estuaries:  
4 relationship to land-derived nitrogen loads and effect of light limitation imposed by algae, *Mar*  
5 *Ecol-Prog Ser*, 247, 59-73, 2003.
- 6 Harvey, G. R., Boran, D. A., Chesal, L. A. and Tokar, J. M.: The structure of marine fulvic and  
7 humic acids, *Mar Chem*, 12, 119-132, 1983.
- 8 Hayn, M., Howarth, R., Marino, R., Ganju, N., Berg, P., Foreman, K., Giblin, A., and  
9 McGlathery, K.: Exchange of nitrogen and phosphorus between a shallow lagoon and coastal  
10 waters. *Estuaries and Coasts* 37, 63-73, 2014.
- 11 Heck, K. L., Able, K. W., Roman, T. C., and Fahay, M. P.: Composition, abundance, biomass,  
12 and production of macrofauna in a New England estuary: Comparisons among eelgrass meadows  
13 and other nursery habitats, *Estuaries*, 18, 379-389, 1995.
- 14 Helms, J. R., Stubbins, A., Ritchie, J. D., Minor, E. C., Kieber, D. J., and Mopper, K.:  
15 Absorption spectral slopes and slope ratios as indicators of molecular weight, source, and  
16 photobleaching of chromophoric dissolved organic matter, *Limnol Oceanogr*, 53, 955-969, 2008.
- 17 Hemminga, M. A., and Mateo, M. A.: Stable carbon isotopes in seagrasses: variability in ratios  
18 and use in ecological studies, *Mar Ecol-Prog Ser*, 140, 285-298, 1996.
- 19 Hoge, F. E., Vodacek, A., and Blough, N. V.: Inherent optical properties of the ocean: Retrieval  
20 of the absorption coefficient of chromophoric dissolved organic matter from fluorescence  
21 measurements, *Limnol Oceanogr*, 38, 1394-1402, 1993.
- 22 Hood, E., Williams, M. W., and McKnight, D. M.: Sources of dissolved organic matter (DOM)  
23 in a Rocky Mountain stream using chemical fractionation and stable isotopes, *Biogeochemistry*,  
24 74, 231-255, 2005.
- 25 Huang, W., and Chen, R. F.: Sources and transformations of chromophoric dissolved organic  
26 matter in the Neponset River Watershed, *J Geophysical Research*, 114, G00F05, 2009.

- 1 Kaldy, J. E., Cifuentes, L. A., and Brock, D.: Using stable isotope analyses to assess carbon  
2 dynamics in a shallow subtropical estuary, *Estuaries*, 28, 86-95, 2005.
- 3 Keefe, C. W., Boynton, W. R., Standing crop of salt marshes surrounding Chincoteague Bay,  
4 Maryland-Virginia, *Chesapeake Science*, 14, 117-123, 1973.
- 5 Keith, D. J., Yoder, J. A., and Freeman, S. A.: Spatial and temporal distribution of coloured  
6 dissolved organic matter (CDOM) in Narragansett Bay, Rhode Island: Implications for  
7 phytoplankton in coastal waters, *Estuar Coast Shelf S*, 55, 705-717, 2002.
- 8 Kennish, M. J., Fertig, B. M., and Sakowicz, G. P.: Benthic macroalgal blooms as an indicator of  
9 system eutrophy in the Barnegat Bay-Little Egg Harbor estuary, *Bull N. J. Acad Sci*, 56, 1-5,  
10 2011.
- 11 Kennish, M. J., Fertig, B. M., and Sakowicz, G. P., In situ surveys of seagrass habitat in the  
12 northern segment of the Barnegat bay-Little Egg Harbor estuary,  
13 <http://bbp.ocean.edu/Reports/2011%20Northern%20seagrass%20survey.pdf>, 2013.
- 14 Kirk, J. T. O.: *Light and photosynthesis in aquatic ecosystems*. Cambridge University Press,  
15 Cambridge and New York, 1994.
- 16 Komada, T., Polly, J. A., and Johnson, L.: Transformations of carbon in anoxic marine  
17 sediments: Implications from  $\Delta^{14}\text{C}$  and  $\delta^{13}\text{C}$  signatures, *Limnol Oceanogr*, 57, 567-581, 2012.
- 18 Kouassi, K. M., and Zika, R. G.: Light-induced destruction of the absorbance property of  
19 dissolved organic matter in seawater, *Toxicol Environ Chem*, 35, 195-211, 1992.
- 20 Lalonde, K., Middlestead, P., and Gelinas, Y.: Automation of  $^{13}\text{C}/^{12}\text{C}$  ratio measurement for  
21 freshwater and seawater DOC using high temperature combustion, *Limnol Oceanogr-Meth*, 12,  
22 816-829, 2014.
- 23 McGranahan, G., Balk, D., Anderson, B., The rising tide: assessing the risks of climate change  
24 and human settlements in low elevation coastal zones, *Environ Urban*, 19, 17-37, 2007.
- 25 Mopper, K., Kieber, D. J., and Stubbins, A.: Marine photochemistry of organic matter: processes  
26 and impacts, In *Biogeochemistry of Marine Dissolved Organic Matter* 2nd ed; Hansell, D. A.,  
27 Carlson, C. A., Ed. Academic Press: Boston, pp 389-450, 2015.

- 1 Nelson, N. B. and Siegel, D. A.: The global distribution and dynamics of chromophic dissolved  
2 organic matter, *Ann Rev Mar Sci*, 5, 447-476, 2013.
- 3 Olsen, P. S., and Mahoney, J. B., Phytoplankton in the Barnegat Bay-Little Egg Harbor estuarine  
4 system: Species composition and picoplankton bloom development, *J Coastal Res Special Issue*,  
5 32, 115-143, 2001.
- 6 Parlanti, E., Worz, K., Geoffroy, L., and Lamotte, M.: Dissolved organic matter fluorescence  
7 spectroscopy as a tool to estimate biological activity in a coastal zone submitted to anthropogenic  
8 inputs, *Org Geochem*, 31, 1765-1781, 2000.
- 9 Peterson, B. J., Fry, B., Hullar, M., Saupe, S., and Wright, R.: The distribution and stable carbon  
10 isotopic composition of dissolved organic carbon in estuaries, *Estuaries*, 17, 111-121, 1994.
- 11 Pregnall, A. M.: Release of dissolved organic carbon from the estuarine intertidal macroalga  
12 *Enteromorpha prolifera*, *Marine Biology*, 73, 37-42, 1983.
- 13 Raymond, P. A. and Bauer, J. E.: DOC cycling in a temperate estuary: A mass balance approach  
14 using natural  $^{14}\text{C}$  and  $^{13}\text{C}$  isotopes, *Limnol Oceanogr*, 46, 655-667, 2001.
- 15 Shen, Y., Chapelle, F. H., Strom, E. W., and Benner, R.: Origins and bioavailability of dissolved  
16 organic matter in groundwater, *Biogeochemistry*, 122, 61-78, 2015.
- 17 Spencer, R. G. M., et al.: Photochemical degradation of dissolved organic matter and dissolved  
18 lignin phenols from the Congo River, *J Geophys Res*, 114, G03010, DOI  
19 10.1029/2009JG000968, 2009.
- 20 Stedmon, C. A., Markager, S., and Bro, R.: Tracing dissolved organic matter in aquatic  
21 environments using a new approach to fluorescence spectroscopy, *Mar Chem*, 82, 239-254,  
22 2003.
- 23 Stewart, A. J., and Wetzel, R. G.: Fluorescence : absorbance ratios- a molecular-weight tracer of  
24 dissolved organic matter, *Limnol Oceanogr*, 25, 559-564, 1980.
- 25 Tzortziou, M., Neale, P. J., Osburn, C. L., Megonigal, J. P., Nagamitsu, M., and Rudolf, J.: Tidal  
26 marshes as a source of optically and chemically distinctive colored dissolved organic matter in  
27 the Chesapeake Bay, *Limnol Oceanogr*, 53, 148-159, 2008.

- 1 United States Environmental Protection Agency: National estuary program coastal condition  
2 report, Chapter 3: Northeast national estuary program coastal condition, Barnegat Bay National  
3 Estuary Program, <http://www.epa.gov/owow/oceans/nepccr/index.html>, 2007.
- 4 United States Fish and Wildlife Service National Wetlands Inventory, Ecological Services:  
5 Wetlands Mapper, <http://www.fws.gov/wetlands/data/mapper.HTML>, 2015.
- 6 Wazniak, C., Hall, M., Cain, C., Wilson, D., Jesien, R., Thomas, J., Carruthers, C., and  
7 Dennison, W.: State of the Maryland coastal bays, Maryland Department of Natural Resources,  
8 Maryland Coastal Bays Program, and University of Maryland Center for Environmental Science,  
9 Integration, and Application Network, Annapolis, MD,  
10 <http://www.mdcoastalbays.org/archive/2004/MCB-State-Bay-2004.pdf>, 2004.
- 11 Weishaar, J. L., Aiken, G. R., Bergamaschi, B. A., Fram, M. S., Fujii, R., and Mopper, K.:  
12 Evaluation of Specific Ultraviolet Absorbance as an Indicator of the Chemical Composition and  
13 Reactivity of Dissolved Organic Carbon, *Environ Sci Technol*, 37, 4702-4708, 2003.
- 14 Wieben, C. M., and Baker, R. J.: Contributions of nitrogen to the Barnegat Bay-Little Egg  
15 Harbor Estuary: Updated loading estimates, 19 p., Chapter prepared for the Barnegat Bay  
16 Partnership State of the Bay Technical Report, 2009.
- 17  
18  
19  
20  
21  
22  
23  
24  
25  
26  
27  
28

1  
2  
3  
4  
5  
6  
7  
8  
9  
10  
11  
12  
13  
14  
15  
16  
17  
18  
19

Table 1. Sampling sites and procedures.

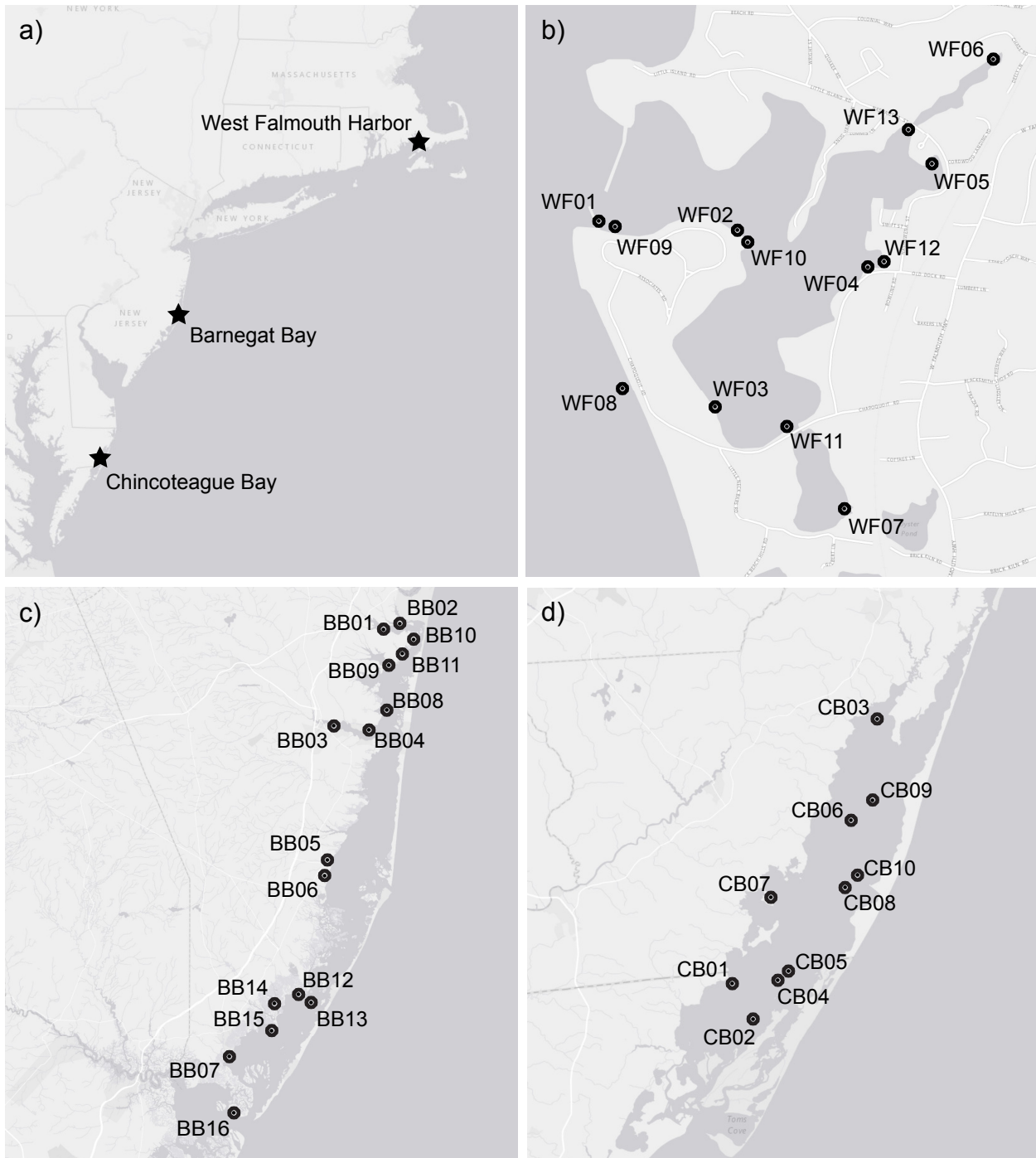
<b>Estuary</b>	<b>No. of sites</b>	<b>Site ID's</b>	<b>Isotope Analysis (Y/N)</b>	<b>Date</b>
West Falmouth Harbor, MA	13	WF01-WF13	Yes	June 25, 2014
Barnegat Bay, NJ	16	BB01-BB16	Yes	July 14-15, 2014
North Barnegat Bay (BB-N)	8	BB01-BB04; BB08-BB11	Yes	July 14-15, 2014
South Barnegat Bay (BB-S)	8	BB05-BB07; BB12-BB16	Yes	July 14-15, 2014
Chincoteague Bay, MD/VA	10	CB01-CB10	No	July 17, 2014



1  
2  
3  
4  
5  
6  
7  
8  
9  
10  
11

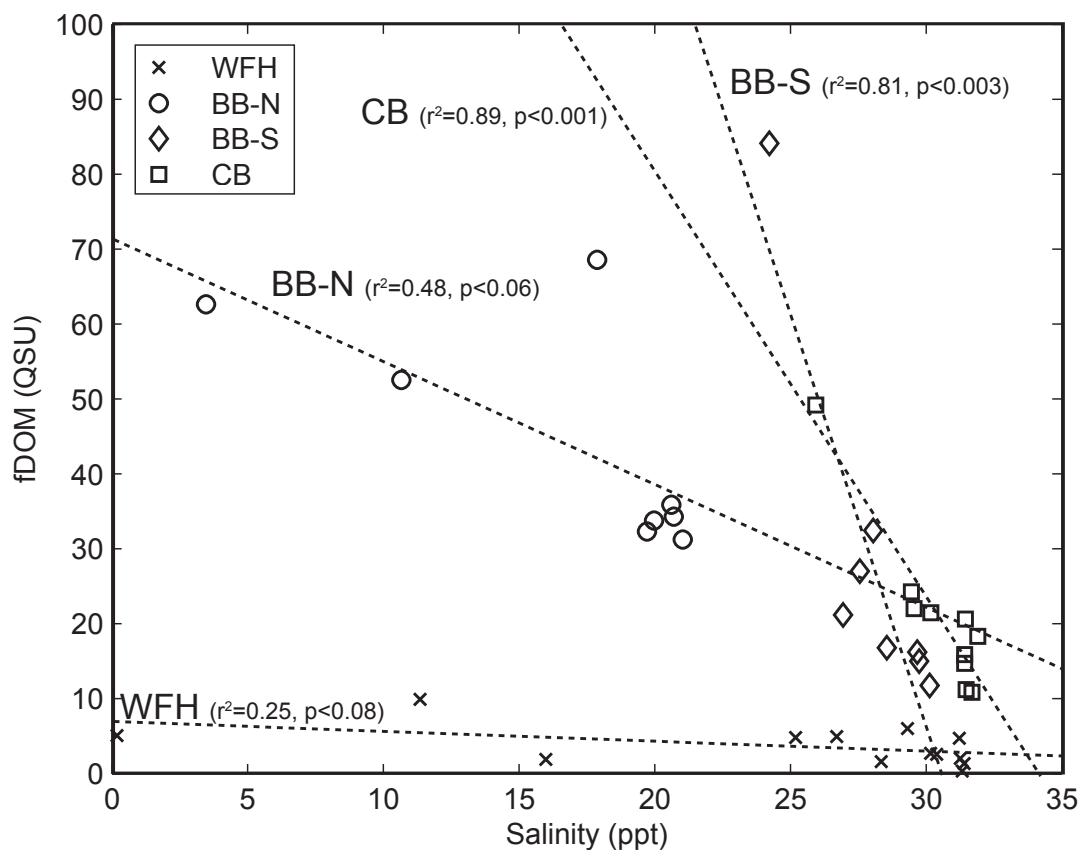
12 Table 2. Light attenuation model parameters and ensuing errors arising from usage of estuary-  
13 wide mean values. Note reduced number of significant figures for reporting of spectral slope as  
14 compared to Table S1.

<b>Estuary</b>	<b>Mean CDOM/fDOM ratio (range)</b>	<b>Mean spectral slope (range)</b>	<b>Mean light attenuation error (range)</b>
West Falmouth Harbor, MA	1.2 (0.50-4.3)	0.03 (0.01-0.05)	15% (0-52%)
Barnegat Bay, NJ	0.23 (0.01-0.96)	0.01 (0.01-0.02)	33% (0-220%)
Chincoteague Bay, MD/VA	0.17 (0.16-0.19)	0.01 (0.01-0.02)	11% (0.01-28%)

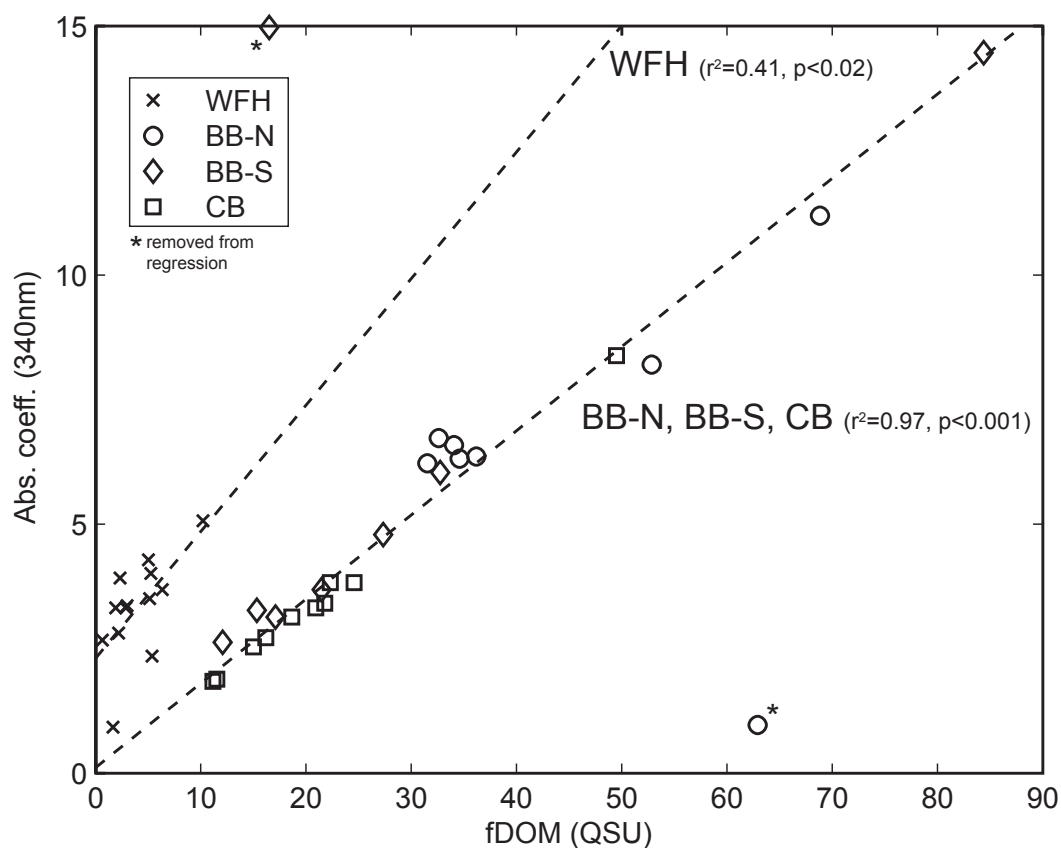


1

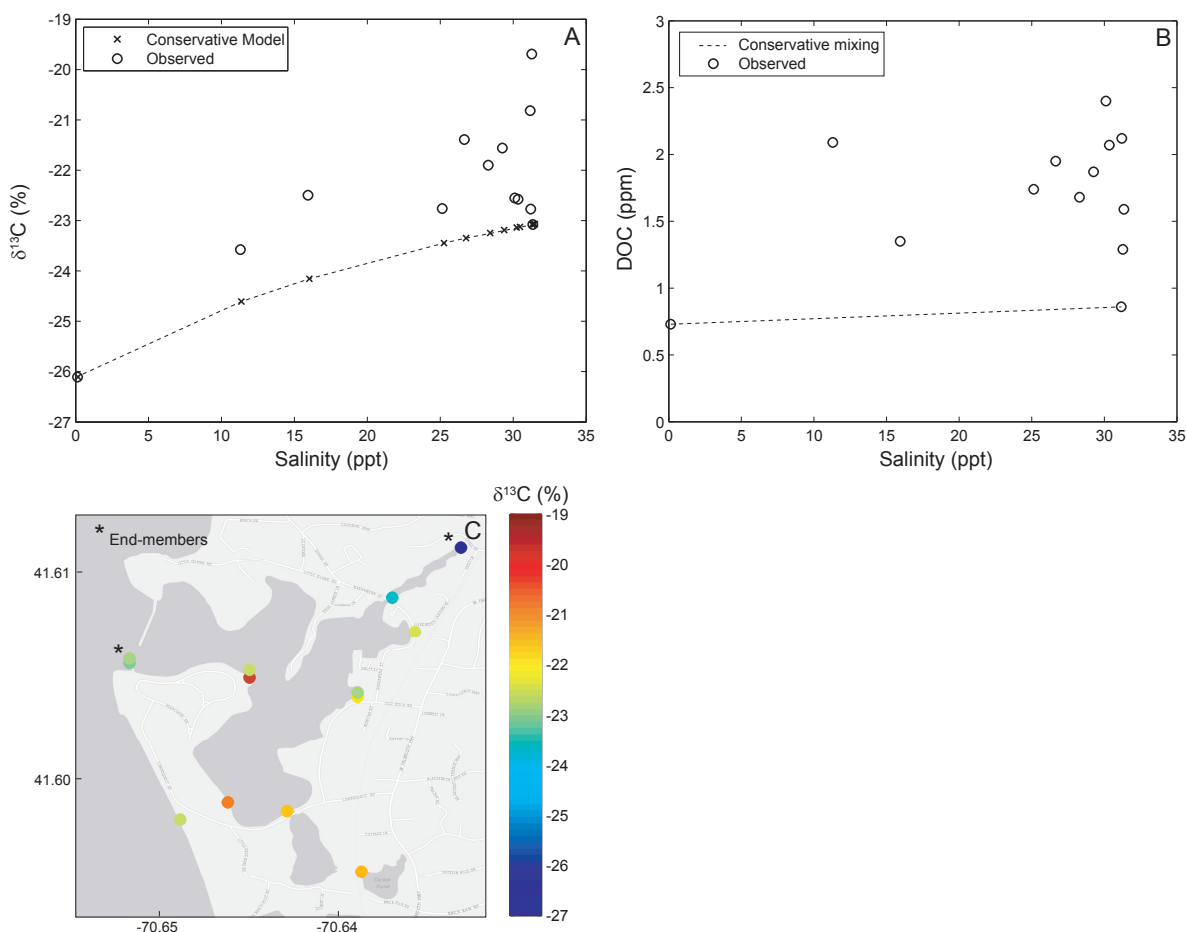
2 Figure 1. (a) Location of U.S. Atlantic Coast estuaries investigated in this study. Sample  
 3 locations within (b) West Falmouth Harbor; (c) Barnegat Bay; (d) Chincoteague Bay.



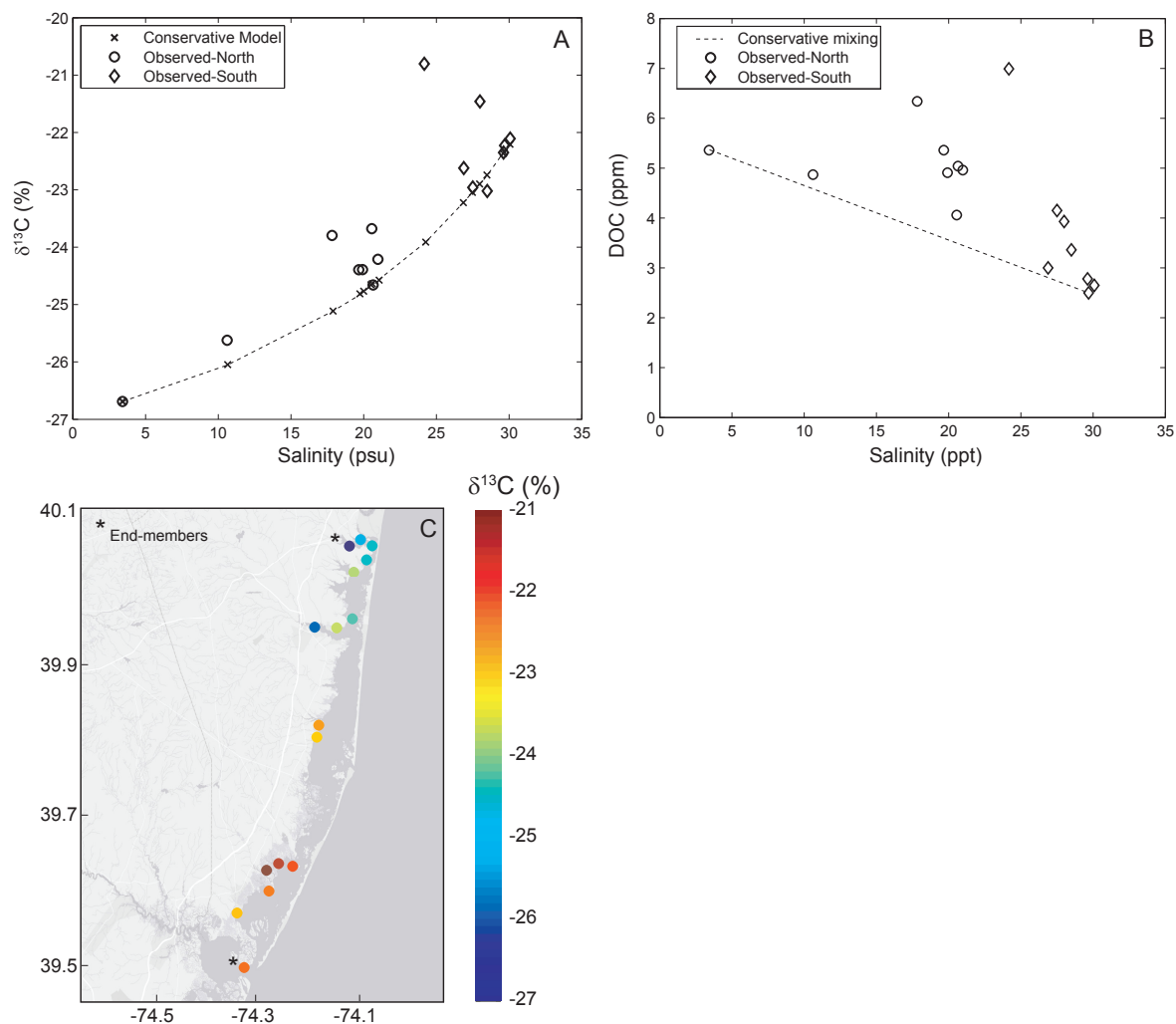
- 1
- 2 Figure 2. Fluorescence measurement versus salinity for all sample sites at West Falmouth Harbor
- 3 (WFH), North Barnegat Bay (BB-N), South Barnegat Bay (BB-S), and Chincoteague Bay (CB).
- 4 Dashed lines indicate the best linear fits to the data, with associated  $r^2$  and  $p$ -value.



1  
 2 Figure 3. Absorption coefficient at 340nm versus fluorescence measurement for all sampling  
 3 sites at West Falmouth Harbor (WFH), North Barnegat Bay (BB-N), South Barnegat Bay (BB-  
 4 S), and Chincoteague Bay (CB). Dashed lines indicate the best linear fit to the data, with  
 5 associated  $R^2$  and p-value. Two outliers (indicated by “\*”) removed from the regressions for  
 6 Barnegat Bay.



1 Figure 4. (a) Measured  $\delta^{13}\text{C}$ -DOC values and salinity for West Falmouth Harbor are plotted  
 2 against an isotopic conservative mixing model for location. Deviations from the model suggest  
 3 contributions of DOC  $^{13}\text{C}$ -enriched relative to the assumed end-members. (b) Measured DOC  
 4 concentration and salinity for West Falmouth Harbor are plotted along with a line of  
 5 concentration-based conservative mixing between end-members. Data points with concentrations  
 6 greater than those predicted by conservative mixing indicate addition of DOM to the system. (c)  
 7 Spatial plot of isotopic signatures measured at West Falmouth Harbor. Asterisks indicate  
 8 assumed end-members.



1 Figure 5. (a) Measured  $\delta^{13}\text{C}$ -DOC values and salinity for both North and South Barnegat Bay are  
 2 plotted against an isotopic conservative mixing model for location. Deviations from the model  
 3 suggest contributions of DOC that is distinct from the assumed end-members. (b) Measured  
 4 DOC concentration and salinity for Barnegat Bay are plotted along with a line of concentration-  
 5 based conservative mixing between end-members. Data points with concentrations greater than  
 6 those predicted by conservative mixing indicate addition of DOM to the system. (c) Spatial plot  
 7 of isotopic signatures measured at Barnegat Bay. Asterisks indicate assumed end-members.

